Application of Wavelet Transform to Extended X-ray Absorption Spectroscopy

H. FUNKE[1,2], M. CHUKALINA[3], A. C. SCHEINOST[1,2]
[1]Institute of Radiochemistry, Forschungszentrum Dresden-Rossendorf, Dresden, Germany
[2]Rossendorf Beamline at ESRF (BM20), Grenoble, France
[3]Institute of Microelectronics Technology RAS, Chernogolovka, Russia
http://www. fzd.de/pls/rois/Cms?pNid=247

Abstract: - A new application of continuous wavelet transform to the data analysis of extended x-ray absorption spectroscopy is presented. The wavelet transform provides not only radial distance resolution of the spectra, but resolves also the wave vector space permitting the discrimination of atoms by their elemental nature. This resolution is especially important if these atoms are at the same distance. The wavelet transform method is applied to a structural problem of Zn-Al layered double hydroxides, demonstrating the homogeneity of the metal cation distribution in the hydroxide layers. Depending on the specific problem, either the well-known Morlet wavelet was used, or a newly developed wavelet, based on theoretical EXAFS back scattering functions.

Key-Words: - Continuous wavelet transform, X-ray absorption spectroscopy, data evaluation

1 Introduction to extended x-ray absorption spectroscopy

Extended X-ray absorption fine structure (EXAFS) spectroscopy is an element-specific probe of the local short range structure of elements in a sample. An important advantage of this technique is its utility for heterogeneous samples. A wide variety of solids and liquids can be examined directly and non-destructively. The absorption energies of the inner electron shells are usually quite high. Therefore the EXAFS technique demands high energy tunable X-rays with high flux and brilliance. As a result, the experiments are usually done at synchrotron radiation facilities.

Since the pioneering work of Stern, Lytle and Sayers to the theory and data analysis of EXAFS spectra [1-4], a fundamental step of the EXAFS data analysis is the discussion of the Fourier transform (FT) of the EXAFS spectra. The modulus of the FT enables a first qualitative estimate of how many coordination shells at which distances are surrounding the absorbing atom. This information is necessary for the subsequent numerical EXAFS analysis, which is performed by fitting the spectrum in either wave vector (k) or Fourier space. The photoelectron wave vector k, the incident photon energy E and the threshold energy E_0 of a particular electronic shell of the atom are related by

$$k = \sqrt{\frac{2m}{\hbar}\left(E - E_0\right)} \qquad (1)$$

where $\hbar$ is Plank's constant and m is the mass of the electron. While the absorbing atom is unequivocally identified by the energy of the absorption edge, the backscattering atoms are identified with limited precision (typically $Z \pm 2$) by a fit to the EXAFS equation based on Fermi's Golden Rule

$$\chi(k) = \sum_{i=1}^{n} \frac{N_i}{R_i^2} \frac{F_i(k,R)}{k} e^{\frac{-2R_i}{\lambda}} e^{-2\sigma_i^2 k^2} \sin(2kR_i + \Psi) \qquad (2)$$

where $\chi(k)$ is the measured EXAFS spectrum. The searched, i. e. fitted, parameters are the number of atoms in the ith coordination sphere N_i, the average radial distance R_i, and the Debye Waller factor σ_i^2. The functions backscattering amplitude $F_i(k,R)$, the sum of the phases of the central- and backscattering atoms $\Psi(k,R)$, and the mean free path $\lambda(k)$ are usually calculated by the FEFF code [5].

FEFF is a commonly used complex computer program for ab initio scattering calculations of EXAFS spectra using predetermined model clusters of atoms. The code yields theoretical scattering amplitudes and phases used in the standard XAFS analysis codes, as well as the EXAFS spectra for each path individually. The identity of the backscattering atom is not fitted and has to be preselected based on the underlying model.

2 Example: Layered Double Hydroxides

Layered double hydroxide (LDH) phases consist of layers of edge-sharing metal hydroxide octahedra, where up to 1/3 of the divalent cations like Co^{2+}, Ni^{2+}, Zn^{2+} (M^{2+}) are replaced by trivalent Al^{3+} [6]. Due to their low crystallinity and turbostratic layer structure, LDH is difficult to determine by x-ray diffraction. While EXAFS is much better suited for this purpose, the localization of the various cations in the structure is complicated by the fact that the backscattering wave from Al^{3+} is masked by destructive interference with backscattering waves from the heavier M^{2+} [7,8]. In [9] one finds a summary to a variety of applications and problems concerning LDH phases.

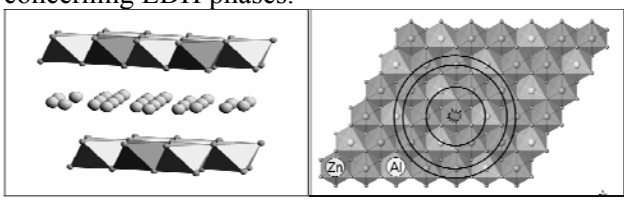

Fig. 1 Scheme and top view of the Model of the octahedral layer of Zn-Al LDH. $Zn(OH)_6$-octahedra are shown in green, $Al(OH)_6$-octahedra are shown in yellow.

The circles in figure1 mark the first three metal shells. Following [10] we assume an even metal distribution in the LDH layer, which is in line with an even charge distribution. In this case, the first metal shell ($r \approx 3.1$ Å = $R_{Zn\text{-}Zn}$) contains 3 Zn and 3 Al atoms, the second metal shell ($r \approx 5.3$ Å = $\sqrt{3} \cdot R_{Zn\text{-}Zn}$), contains 6 Zn atoms, and the third metal shell ($r \approx 6.2$ Å = $2 \cdot R_{Zn\text{-}Zn}$), contains 3 Zn and 3 Al atoms.

The EXAFS spectrum of a Zn-Al LDH were measured at the Rossendorf beamline (ESRF, Grenoble) at T = 20 K in a cryostat to reduce thermal oscillations.

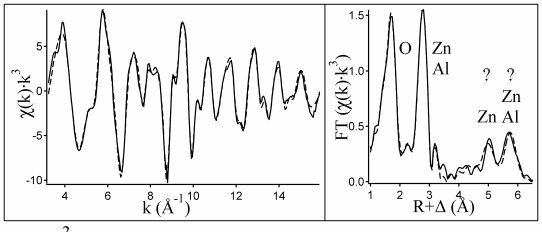

Fig. 2 k^3 weighted Zn *K*-edge EXAFS spectrum and its FT magnitude of Zn-Al LDH. The fit is shown in dotted lines.

The FT magnitude shows four dominant shells, which can be assigned to the oxygen coordination sphere (O), and to the first, second and third sphere of metal (Zn, Al) neighbors (Fig. 1).

3 Wavelet analysis of the EXAFS spectrum of a Zn-Al LDH

The wavelet transform of the k^n weighted EXAFS spectrum is given as [11]:

$$W_\chi^\psi(k,r) = \sqrt{2r} \int_{-\infty}^{+\infty} \chi(k') k'^n \psi^*[2r(k'-k)]\, dk'. \quad (3)$$

Thereby the "mother" wavelet function may be chosen from the wide class of functions l^2 with the zero mean condition as the only restriction.

$\chi(k)$ is the EXAFS signal, and $\psi^*\left[2r(k'-k)\right]$ is the complex conjugated wavelet function, translated by k and dilatated by the distance parameter $2r$. The geometrical meaning of r is explained below.

3.1 Wavelet analysis using Morlet wavelets

3.1.1 Morlet wavelets for EXAFS data analysis

For EXAFS data analysis we have chosen the complex Morlet wavelet as mother wavelet [11].

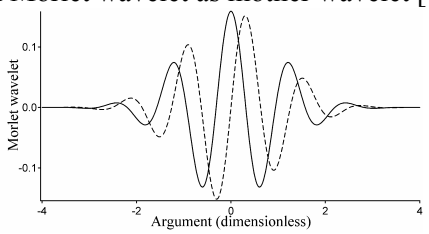

Fig. 3 Real (full line) and imaginary (dashed line) part of the Morlet wavelet for η = 5 and σ = 1.

The Morlet wavelet is obtained by taking a complex sine wave (like in the Fourier transform), and by confining it with a Gaussian.

$$\psi(k) = \frac{1}{\sqrt{2\pi}\sigma} \exp(i\eta k) \cdot \exp\left(\frac{-k^2}{2\sigma^2}\right). \quad (4)$$

If the Morlet parameters fulfill the condition: $\eta\sigma \gg 15$, i.e. if one forms a wavelet containing many oscillations (the "overview wavelet"), the dilatation parameter *r* of the wavelet transform and the distance parameter *R* of the Fourier transform coincide asymptotically. For Morlet parameters in the order of $\eta\sigma \approx 5$ (the "detail wavelet"), we receive a better resolution concerning the wave vector k.

The choice of the Morlet wavelet was based on the fact, that its structure is similar to an EXAFS signal with a slowly varying amplitude term and a fast oscillating phase term. The parameters η and σ are sufficiently descriptive to be adapted easily to the present problem, e.g. to identify different elements at a given distance of the central atom.

Limitations of the resolution of a wavelet transform with Morlet wavelets are given by their uncertainty (Heisenberg) boxes (see e.g. [12,13]):

$$\left[k-\frac{\eta\sigma}{\sqrt{2}r},k+\frac{\eta\sigma}{\sqrt{2}r}\right]\times\left[r-\frac{r}{\sqrt{2}\eta\sigma},r+\frac{r}{\sqrt{2}\eta\sigma}\right]. \quad (5)$$

From relation (5) follows that the $k-r$ window is narrow in k space for large values of r, and is wide for small r. The resolution in r space hence decreases with increasing r. On the other hand, for large values of the product of the Morlet parameters $\eta\sigma$ the uncertainty is large for k and small for r and vice versa. Therefore, the resolution in k and r critically depends on the selection of the Morlet parameters η and σ. It is marked that the uncertainties fulfill the relation $\Delta_k\Delta_r = 1/2$.

3.1.2 Analysis of the Zn-Al LDH phase using Morlet wavelets

Figure 4 shows the overview wavelet transform of the Zn-Al LDH with a signal weighting of k^3. The peak at r = 1.7Å corresponds to the oxygen coordination shell. The peaks at r = 2.8, 5.0 and 5.8 Å correspond to the first, second and third metal shells with distances corresponding to the FT (see figure 2). However, the different Zn and Al back scatterer, which are contained in this shells, are not resolved along k.

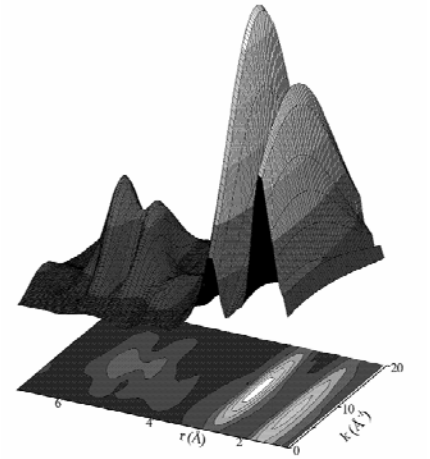

Fig. 4 Overview wavelet transform with Morlet parameters η = 15, σ = 2

Figure 5 shows the detailed wavelet transform of the first metal shell at r = 2.8 Å with Morlet parameters η = 30, σ = 0.184. The wavelet ridge at r ≈ 2.8 Å is clearly resolved and shows two peaks at different k. The peaks demonstrate the existence of two different back scatterer in the first metal shell, the easier aluminum and the heavier zinc. This result is clear, because the resolution conditions (5) for k and r are both fulfilled for the first metal shell.

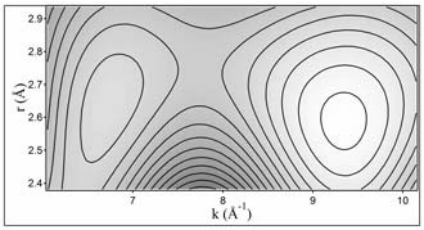

Fig. 5 Detail wavelet transform with Morlet parameters η = 30, σ = 0.184.

For the second and third metal shell, however, the resolution condition is fulfilled either only for r in the overview wavelet transform or is fulfilled only for k in the detail wavelet, see figure 6.

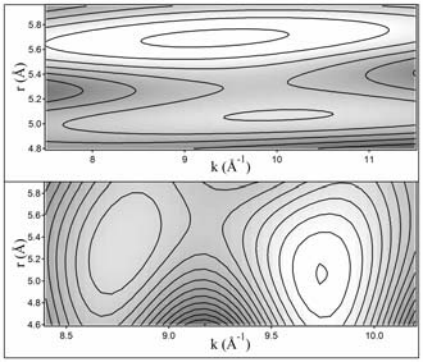

Fig. 6 Overview wavelet transform with Morlet parameters η = 30, σ = 1 at top and detail wavelet transform with Morlet parameters η = 30, σ = 0.155 at bottom.

The overview wavelet transform shows two shells clearly discriminated in r in complete agreement with the Fourier transform (see figure 2), while the resolution in k is not sufficient to resolve the two types of atoms. In reverse, the detail wavelet transform shows two shells clearly discriminated in k, but the resolution in r is not sufficient to resolve the two different distances. Hence the simultaneous resolution in r and k space of the third and fourth metal shells is impossible using the Morlet wavelet. The presence of both elements, aluminium and zinc, in both back scattering shells is proven, but not the regular distribution of the metal ions, as it was assumed in figure 1.

To overcome this limitation we have developed a new especially adapted mother wavelet, which is described in the following sections.

3.2 Wavelet analysis using FEFF-Morlet wavelets

3.2.1 Generation of FEFF-Morlet wavelets

When analyzing complex signals with wavelet transform, we have to discriminate two cases. In case one, neither a basic theory nor a mathematical model exist, which could be applied to the process under investigation. An example are the EEG signals of the human brain, where time-frequency plots of the electrical current measured in response to different events are treated as fingerprints of these events. Even without a basic theory, this wavelet method is widely used for medical diagnostics and has largely replaced Fourier analysis. In case two, an at least rudimentary mathematical model of the process under investigation exists. The model or parts of it may then be used to construct a wavelet specifically adapted to the process. An example is seismic oil prospection, where the reflexion of pressure waves on single sediment boundaries can be modeled, while the description of the complex reflexion processes across greater depths of the Earth's crust fails.

EXAFS spectra can be considered as belonging to this second group, since the spectra may be modeled by the EXAFS equation, see formula (2).

In our new model, EXAFS functions for selected paths calculated with the FEFF8.2 program [5], form the basis for the construction of mother wavelet functions. Wavelets, designed in this way, should be in good agreement with individual paths of interest, which are contained in the experimental spectrum. Thus the sensitivity of the wavelet transform for these paths is strengthened. In comparison to such real functions, complex mother wavelet functions, like Morlet or Cauchy wavelets, generate much more descriptive plots of magnitude. Thus, taking the FEFF designed wavelet as real part, the associated imaginary part has to be constructed. The sum of the real and the imaginary parts form the FEFF-Morlet wavelet. This wavelet is expected to combine the accurate characteristics of the theoretical EXAFS function with the descriptiveness and simplicity of the complex Morlet wavelet.

We propose to generate FEFF-Morlet mother wavelets in five steps. A detailed description of the procedure is given in [14].

1) Modeling a spectrum using a special FEFF path and build the envelopes with a spline function,
2) Adapt the EXAFS oscillations within the envelopes to the cosine function, which results in the real part of the wavelet,
3) Add the same function with a phase shift of π/2, which results in the imaginary part of the wavelet,
5) Set the "center of gravity" of the curve to zero.

3.2.2 Analysis of the Zn-Al LDH phase using FEFF-Morlet wavelets

Following the proposed procedure four FEFF-Morlet wavelets have been constructed. They are based on the single scattering paths Zn-Al @ 5.3 and 6.2 Å with the Debye-Waller factor $\sigma^2 = 0.0056$ Å^2, and Zn-Zn @ 5.3 and 6.2 Å with $\sigma^2 = 0.0065$ Å^2. The resulting wavelets are shown in Fig. 7.

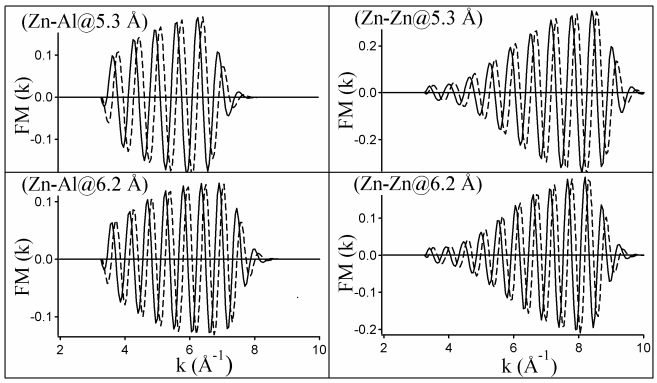

Fig. 7. Real (full) and imaginary (dashed) part of the FEFF-Morlet wavelets FM (*k*) constructed from the four model spectra.

Owing to its construction the FEFF-Morlet wavelet is the optimal mother wavelet function for a specific backscattering atom at a specific distance. The information about the optimal distance is contained in the FEFF-Morlet wavelet $\psi^{FM}_{[r_{opt}]}$ itself. Each scaling (stretching or shrinking) would mean a decrease of the agreement, if the basis model is correct.

Consequently, the dilatation parameter *r* is replaced by a new scale parameter *s* if the mother wavelet is a function derived from a certain model. The definition of *s* is, that *s* = 1, if the argument of the wavelet is not scaled. It means, if the wavelet transform for *s* = 1 (in a certain region of *k*) shows a maximum, then the signal and the mother wavelet function in this *k* region coincide maximally.

The wavelet transform (2), depending on the translation and scale parameters *k* and *s*, then takes the form:

$$W^{\psi}_{\chi}(k,s) = \sqrt{s}\int \chi(k')\,k'^{3}\,\psi^{FM*}_{[r_{opt}]}[s(k'-k)]dk' \quad (6)$$

In order to focus the wavelet transform analysis to specific distances, the power density function $\Phi(s) = \int \left[W_\chi^\psi (k,s) \right]^2 dk$ is introduced. The calculation of $\Phi(s)$ is performed by integration over the entire *k* range of the experimental spectrum.

Now the FEFF-Morlet technique is applied to verify the model of Brindley & Kikkawa [10], assuming an even metal distribution in the LDH layer, in line with an even charge distribution (see figure 1). The wavelet transform analysis of the second and third metal shell of the LDH spectrum will be performed using the four FEFF-Morlet wavelet mother functions pictured in figure 7.

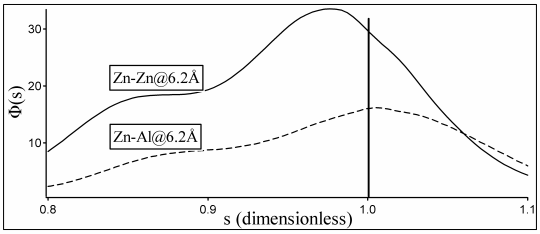

Fig. 8: Two power density functions *Φ(s)* of the wavelet transform of Zn-Al LDH, performed with the adapted FEFF-Morlet wavelets (see text).

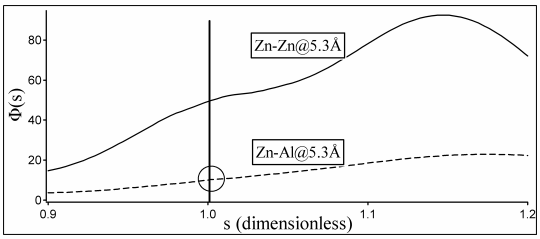

Fig. 9 Two power density functions *Φ(s)* of the wavelet transform of Zn-Al LDH, performed with the adapted FEFF-Morlet wavelets (see text).

For $r \approx 6.2$ Å, the analysis of the wavelet transforms with the power density function *Φ(s)* shows maxima around $s = 1$ for Zn and Al, confirming that both atoms are present at this distance (Fig.11). At a distance of $r \approx 5.3$ Å, however, only the path involving Zn backscattering shows an additional shoulder at $s = 1$, while the path involving Al does not (circle) (Fig. 12). This confirms the model shown in Fig. 1.

4 Conclusion

By the example of a Zn-Al LDH it was demonstrated that the application of the wavelet approach to EXAFS data analysis is well suited to distinguish two different atoms at similar distances. With the previously used Morlet wavelet, it was possible to distinguish Zn and Al in the first metal shell (≈ 3.1 Å) of the LDH spectrum. However, it was not possible to resolve the two more distant shells at 5.3 and 6.2 Å simultaneously with respect to wavenumber *k* (element identity) and the distance *r*. This problem is now overcome with the newly developed FEFF-Morlet wavelet. FEFF-Morlet wavelets were individually adapted to resolve the second and third metal shell of Zn-Al LDH. We were now able to show that the second metal shell contains only Zn, and the third metal shell both Zn and Al.

In this study we made use of the most important advantage of the continuous wavelet transform, the possibility to permit infinitely many test functions from the function class l^2. The FEFF-Morlet wavelet is a sharper, however also more complicated, instrument for EXAFS data analysis than the Morlet wavelet.

References:

[1] Sayers D. E., Stern E. A., *Phys. Rev. Lett*, **27**, 1971, 1204-1207.
[2] Stern E. A., *Phys. Rev. B***10**, 1974, 3027- 3037.
[3] Lytle F. W., Sayers D. E., Stern E. A., *Phys. Rev. B*, **11**, 1975, 4825-4835.
[4] Stern E. A., Sayers D. E., Lytle F. W., *Phys. Rev. B*, **10**, 1975, 4836-4846.
[5] Ankudinov A. L., Ravel B., Rehr J. J., Conradson S. D. *Phys. Rev. B***58**, 1998, 7565-7576.
[6] Voegelin A., Scheinost A. C., Bühlmann K., Barmettler K., Kretzschmar R., *Environ. Sci. Technol.* **36**, 2002, 3749-3754.
[7] Manceau A. (1990). Can. Mineral., **28**, 321-328.
[8] Scheinost, A. C., Ford R. G., Sparks D. L. (1999). *Geochim. Cosmochim. Acta*, ***63***, 3193-3203.
[9] Duan X., Evans D.G., Editors, Structure and Bonding, Vol. 119, *Layered Double Hydroxides*, Berlin Heidelberg, Springer, 2006.
[10] Brindley G. W. & Kikkawa S. *Am. Mineral.* **64**, 1979, 836-843.
[11] Funke H., Scheinost A.C. & Chukalina M. *Phys. Rev. B***71**, 2005, 094110.
[12] Chui C. K., *An Introduction to Wavelets*, Academic Press, San Diego, London, 1992.
[13] Louis A. K., Maas P. and Rieder A., *Wavelets: Theory and Applications,* Wiley, N Y, 1997.
[14] Funke, H., Chukalina, M., Scheinost, A. C., J. Synchrotron Rad. **14**, 2007, 426-432.